Structure and Stability of M−CO, M = First-Transition-Row Metal: An Application of Density Functional Theory and Topological Approaches

Julien Pilme and Bernard Silvi*

Laboratoire de Chimie Théorique (UMR-CNRS 7616), Université Pierre et Marie Curie, 4 Place Jussieu 75252-Paris cédex, France

Mohammad Esmail Alikhani

Laboratoire de Dynamique, Interactions et Réactivité (UMR-CNRS 7075), Université Pierre et Marie Curie, 4 Place Jussieu 75252-Paris cédex, France

Received: October 14, 2002; In Final Form: March 24, 2003

The nature of the bonding in the binary transition-metal carbonyl complex has been analyzed by topological approaches (atoms in molecules (AIM) and electron localization function (ELF)) from a series of calculations carried out at the hybrid Hartree−Fock/DFT level (B3LYP). It is shown that the interaction between a transition metal and CO should be characterized as a dative bond, in which the monosynaptic basin of the carbon plays the role of the disynaptic basin connecting the metal core to the carbon atom. For all atoms except Cr, Mn, and Cu, the multiplicity of the ground state is given by applying Hund's rule to the maximal core occupancy (i.e., [Ar]c^{n+2}): high-spin complexes for $n < 4$, low-spin for $n > 5$, spin-conserved for $n = 4, 5, 9$. The charge transfers and the spin density on the ligand are rationalized by resonance structures of the same multiplicity. In all complexes except CrCO and CuCO, the ELF function in the core has a local cylindrical symmetry that in turn favors a linear structure; moreover, 2 electrons are available for the charge transfer toward the CO moiety and for the metal nonbonding valence basin. In CrCO and CuCO whose cores have a spherical symmetry, only one electron can be shared by the net transfer and the nonbonding valence basin. The maximization of the charge transfer implies a bent geometry. Finally, we propose two new donation−back-donation schemes based on the AIM and ELF partitions. In the ELF framework, the net charge transfer is almost equal to the π back-donation, the σ-donation being negligible.

1. Introduction

The bonding between transition-metal atoms and carbon monoxide is of considerable interest as a basic model for both molecular and surface chemistry. Among small transition-metal complexes, metal−monocarbonyls, M−CO, have been extensively studied both experimentally[1−13] and theoretically.[14−28] The previous reviews of the theoretical works carried out on these compounds focused on the energetic and bonding properties from the orbital point of view. One of the most puzzling features of the M−CO bonding is that the stabilization energy ranges from few kcal. mol^{-1} to typical dative bond values, c. a. ∼50 kcal. mol^{-1}, according to the nature of the transition metal. Up to now most descriptions of the bonding of the M−CO complexes, where M is a transition metal, rely on the traditional picture of Dewar, Chatt, and Duncanson (DCD).[29,30] This model is based on a balance between σ donation from the carbonyl (the carbon lone pair) to the vacant orbital of the metal atom and π back-donation from the metal to the CO π^* orbital. Recently, two systematic theoretical works[21,25] have been published on the first-row transition-metal monocarbonyl features using the DCD scheme. The main objective of these papers on the M−C bonding was to understand the following points:

(i) All complexes have a $C_{\infty v}$ symmetry except two cases, Cr−CO and Cu−CO, which have a bent structure in the ground state,

(ii) The metal atom always bears a positive charge[25]

(iii) There is no any unique scheme to describe the M−CO bonding. Several mechanisms have been proposed to describe the ground-state symmetry of these systems: (i) 4s to 3d promotion; (ii) spin pairing promotion; (iii) 4s to 3d$_\sigma$ hybridization; (iv) bending. Nevertheless, the bent geometry for Cr− and Cu−CO remains as an exception along the whole series.

In this paper, we have applied the topological analysis of the electron localization function (ELF) to explain the electronic structure and the geometry of the M−CO complexes and to derive simple rules based on the topological properties of this latter function.

For many complexes the lowest energy levels belonging to the different spin multiplicities lie in a rather narrow window; consequently, there are contradictions even in recent theoretical works, for example, in the case of Mn−CO.[21,22,25] To obtain a reliable set of molecular properties, we have first investigated the basis set effects, which are shown to be of primary importance for the determination of the adiabatic binding energy. However, we should note that the geometrical parameters of the studied complexes in a given electronic state do not depend on the level of theory (vide infra).

2. Results and Discussion

All the calculation have been performed with the Gaussian 98/DFT quantum chemical package.[31] The DFT calculations have been carried out with Becke's three-parameter hybrid

* Corresponding author. E-mail: silvi@lct.jussieu.fr.

10.1021/jp027203p CCC: $25.00
Published on Web 05/06/2003

TABLE 1: Energetic Separations (kcal/mol) of the Ground State and the Excited State Correlated with the M−CO Ground State Multiplicity and Symmetry[a]

	6-311G(2d)	6-311G+(2d)	TZV	SDD	exp
Sc ^{2}D−^{4}F	34.9	21.2	21.2	23.8	32.9
Ti ^{3}F−^{5}F	20.8	4.5	10.8	9.1	18.7
V ^{4}F−^{6}D	19.4	43.7	1.5		6.0
Fe ^{5}D−^{3}F	49.5	21.4	55.3	22.2	34.2
Co ^{4}F−^{2}F	33.4		8.4	20.7	21.3
Ni ^{3}D−^{1}S	42.3	54.0	31.9	35.8	41.5

[a] It has not been possible to calculate either the ^{6}D state of V with SDD or the ^{2}F state of Co with 6-311G+(2d).

method[32] using the Lee−Yang−Parr correlation functional[33] (denoted as B3LYP). We have used the 6-311+G(2d) extended basis set[34−36] for the carbon and oxygen atoms. Several basis sets have been used for the first series of transition metals: 6-311+G(2d), 6-311G(2d), TZV,[37,38] and SDD[39] (with Stuttgart pseudopotential for 10 core electrons, and the (8s7p6d1f)/[6s5p3d1f]-GTO contraction scheme for valence (3s3p3d4s) electrons). The bonding between the transition-metal atom and carbonyl units is investigated using the topology of the electron localization (ELF).[40] The topological analysis has been carried out using the TopMod package.[41]

2.1. Structural Analysis. In the $3d^n4s^2$ electronic configuration, the transition metals form van der Waals complexes with the carbon monoxide molecule because the large Pauli repulsion arising from the metal valence shell hampers the formation of a true chemical bond. This is the case of all first series of transition metals in their ground state except for Cr and Cu. The formation of a chemically bonded complex involves the $3d^{n+1}4s^1$ configuration of the metal atom, which is usually its first excited state, except for Cr and Cu for which it is the ground state. The energetic separation between the excited and ground states of the first row transition metals are experimentally known (Table 1). It is a rather difficult task to reproduce accurately the energetic separation between these two states by quantum chemical methods (see ref 20 for a detailed discussion). In fact, such a calculation is strongly basis set dependent, and therefore it is very important to select the basis set that yields the best results. It is the reason we have used four different basis sets for transition metals: 6-311G(2d) (labeled as BS1), 6-311+G(2d) (labeled as BS2), TZV (labeled as BS3), and SDD (labeled as BS4). For a pragmatic point of view the "best" basis set for a metal should fulfill the following requirements:

(i) for a given multiplicity the convergence is achieved on the expected electronic configuration (e.g., $3d^n4s^2$ vs $3d^{n+1}4s^1$),

(ii) the calculation yields the correct ordering of the two lowest atomic configurations, and

(iii) the order of magnitude of the energetic separation between these latter space is accounted for.

It is worth noting that basis set effects are mostly responsible for discrepancies between calculations and experiments because numerical tests carried out with several post Hartree−Fock correlation schemes (MP*n*, CCSD(T)) or with different exchange-correlation functionals (BPW91, B3LYP) show that the correlation treatment *never* corrects these discrepancies.

Because the $3d^{n+1}4s^1$ configuration is the only one able to react with CO, for each transition-metal atom we have to choose a basis set that provides this configuration. Owing to these points, the BS1 basis was selected for Sc and Ti, the BS2 basis for Mn and Fe, the BS3 basis for V, and BS4 basis for Cr, Co, Ni, and Cu atoms. In the case of carbon monoxide, the best agreement with spectroscopic results has been obtained with the BS2 basis set. Diffuse functions noticeably improve the molecular properties of CO. In the following, we present thus the calculated results with the above selected basis sets. We emphasize that with these basis sets, the first excited spin−orbital configuration of each metal is very well reproduced with respect to the experimental data.

TABLE 2: Structural Parameters of the Studied Compounds

	state	r_{CO} (Å)	r_{MC} (Å)	∠MCO (deg)	BDE[a] (kcal/mol)
ScCO	$^4\Sigma^-$	1.166	2.070	180.0	49.7
	$^2\Pi$	1.143	2.202	180.0	41.3
TiCO	$^5\Delta$	1.159	2.021	180.0	45.3
	$^3\Delta$	1.171	1.924	180.0	28.0
VCO	$^6\Sigma^+$	1.150	1.994	180.0	26.6
	$^4\Delta$	1.167	1.909	180.0	13.8
CrCO	$^7A'$	1.143	2.216	137.2	5.8
	$^7\Sigma^+$	1.133	2.206	180.0	2.9
MnCO	$^6\Pi$	1.151	2.037	180.0	22.8
	$^4\Pi$	1.151	1.920	180.0	17.5
FeCO	$^3\Sigma^-$	1.149	1.774	180.0	19.3
	$^5\Sigma^-$	1.144	1.923	173.4	17.0
CoCO	$^2\Delta$	1.147	1.726	180.0	51.8
	$^4A'$	1.142	1.922	153.0	14.6
NiCO	$^1\Sigma^+$	1.149	1.672	180.0	27.8
	$^3A'$	1.142	1.910	144.0	14.3
	$^3\Delta$	1.131	1.928	180.0	9.1
CuCO	$^2A'$	1.141	1.952	138.9	8.7
	$^2\Sigma^+$	1.128	1.952	180.0	4.1

[a] BDE = bond dissociation energy = $[E_{CO} + E_M(3d^{n+1}4s^1(\uparrow))] - E_{complex}$.

Different spin multiplicities in the linear or bent geometries have been calculated for each compound to determine the global minimum of the M−CO system. Structural properties of the M−CO complexes are reported in Table 2, for the ground and first excited states of each complex. It is worth noting that the optimized geometries are far from sensitive to basis set and correlation schemes, as testified by the literature.[22,25,42,50]

We have calculated the bond dissociation energy (BDE) with respect to the first excited state of metal and ground state of CO:

$$\mathrm{BDE} = (E(\mathrm{M}(3d^{n+1}4s^1)) + E(\mathrm{CO})) - E(\mathrm{MCO})$$

Cr− and Cu−CO Complexes. The bond dissociation energies were calculated to be −5.8 and −8.7 kcal/mol for Cr−CO and Cu−CO, respectively. Both complexes were detected in matrix at low temperature,[2,42−44] whereas only Cu atoms were found to be reactive with respect to complex formation with CO at room temperature.[45,46] The Cr−CO singularity was explained by a weakest π-bonding interaction, because the single occupancy of the d_π orbitals.[47]

From electron spin resonance (ESR) experiments, the Cu−CO complex was found to be linear ($^2\Sigma$ electronic state),[48] whereas the theoretical investigations proposed a bent structure.[22,24,27] Barone using DFT calculations showed that the linear Cu−CO corresponds to a transition state.[24] In recent experimental works, the three fundamental vibrational modes, namely, the CO and MC stretching modes (ν_{CO} and ν_{MC}) and the bending mode δ_{MCO}, were identified with the help of isotopic effects and it has been evidenced that the Cu−CO complex has actually a bent geometry.[2,42] Our prediction on the Cu−CO compound is in line with previous theoretical works.

The calculated bond dissociation energy for Cu−CO, corrected for BSSE and ZPE effects, is in good agreement with the experimental data[45] (7.9 vs 7.0 kcal/mol). In the case of Cr−CO, the bond dissociation energy after BSSE and ZPE corrections was found to be 5.3 kcal/mol, slightly less stable

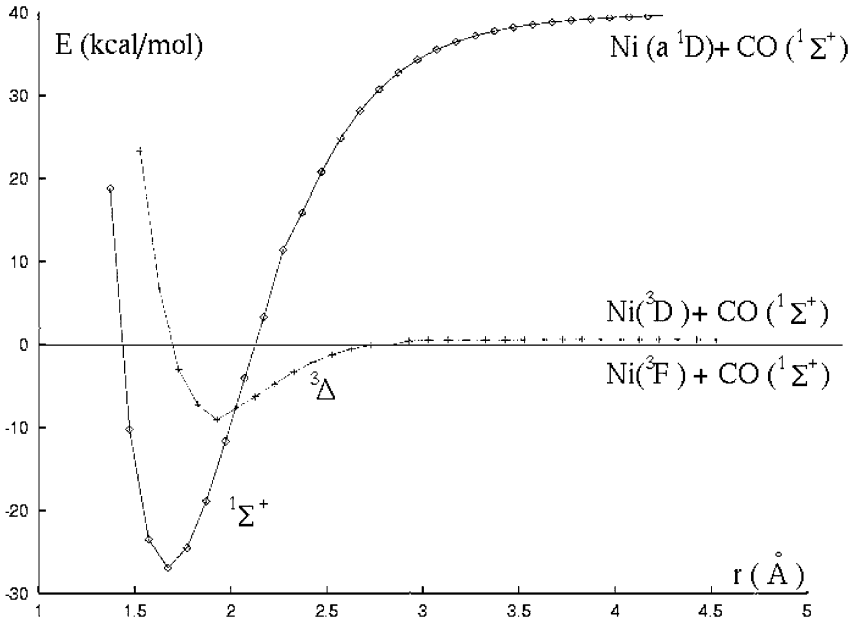

Figure 1. Intersystem crossing between the $^3\Delta$ and $^1\Sigma^+$ curves of Ni−CO.

than Cu−CO. In addition, the Cr−C bond is weaker than the Cu−C one: the Cu−C bond length is by 0.124 Å shorter than that of Cr−C, and the force constant of Cu−C is stronger than the Cr−C one (0.95 vs 0.25 mdyne/Å).

The MCO bond angle was calculated to be around 139°. Because this value is much smaller than 180°, we can conclude that the bent structure cannot be due to a Jahn Teller effect. In addition, the unpaired electron in the linear Cu−CO has a σ character ($\rho(s)_{Cu}$ = 82% vs 0.79 ESR value[4]) that excludes a degenerate state ($^2\Pi$).

Mn−CO Complex. Among all monocarbonyl complexes, Mn−CO seems to play a particular role. Although Huber et al., for the first time, tentatively assigned the 1850 cm^{-1} band observed in the argon matrix to the CO stretching mode of Mn−CO,[49] similar study by Weltner et al.[44] did not allow this band to be identified. Finally, in the Andrews's group,[50] a band localized at 1950.7 cm^{-1} was assigned to the same CO stretching mode of Mn−CO, when laser-ablated metal atoms were co-deposited with carbon monoxide in solid neon.

The available theoretical results are not always consistent among themselves. Fournier,[20] using a pure BP functional, found the $^6\Pi$ and $^4\Pi$ unbound, with the $^6\Pi$ state 8 kcal/mol above the $^4\Pi$ state. Adamo,[25] using a hybrid B3LYP functional, calculated the $^4\Pi$ state as ground state with a bond dissociation energy of 16.4 kcal/mol with respect to Mn(^{6}S 3d^{5}4s^2) + CO($^1\Sigma$). Bauschlicher,[51] using a high-correlated method (ICACPF), found the $^6\Pi$ state as the ground state, but the bond dissociation energy was not calculated.

Our calculations, using the B3LYP/BS2 method, give the two excited states (a ^{6}D 3d^{6}4s^1 and a ^{4}D 3d^{6}4s^1) with a separation of about 4900 cm^{-1} for atomic Mn. The error is 22%, compared to the experimental value. For the Mn−CO complex, it has been found that the $^6\Pi$ state is 5.3 kcal/mol below the $^4\Pi$ state, whereas the $^6\Pi$ bond dissociation energy was found to be 22.8 kcal/mol, with respect to the Mn(a ^{6}D 3d^{6}4s^1) + CO($^1\Sigma$) asymptote. Our calculated $^6\Pi-^4\Pi$ separation (5.3 kcal/mol) is close to that found by Bauschlicher[51] (7.5 kcal/mol). Nevertheless, the $^6\Pi$ state is 26.0 kcal/mol above the ground state of Mn(a ^{6}S 3d^{5}4s^2). We note that our geometrical parameters are very close to those of ref 51 (r_{CO} = 1.150 and r_{MC} = 2.037 Å to be compared to 1.158 and 2.025 Å for $^6\Pi$ state). In line with the results obtained with the ICACPF approach,[51] the C−O bond length is nearly the same for two states, whereas the Mn−C distance in the $^4\Pi$ state is shorter than that in the $^6\Pi$ state. Owing to the energetic properties of the Mn−CO complex, it could be considered as a frontier complex between the high-spin and low-spin compounds.

Low-Spin Complexes. The first excited states of Ni, Co and Fe are ^{3}D (3d^9(^{2}D)4s^1), b ^{4}F (3d^8(^{3}F)4s^1), and a ^{5}F (3d^7(^{4}F)-4s^1), respectively. As shown in Table 2, the M−CO compounds in these excited states (high spin) are always above the low-spin compounds, namely, Ni−CO($^1\Sigma^+$), Co−CO($^2\Delta$), and Fe−CO($^3\Sigma^-$).

For these compounds, an intersystem crossing occurs between the high- and low-spin states, which could be avoided by off-diagonal spin−orbit matrix elements. In the case of Ni−CO, as illustrated in Figure 1, intersystem crossing occurs near the equilibrium position of the $^3\Delta$ state of Ni−CO, which allows the complex to be stabilized in the$^1\Sigma^+$ state.

We turn now to the Fe−CO complex. The two$^3\Sigma^-$ and$^5\Sigma^-$ states dissociate to the Fe(d^{7}s^1) configuration. In line with a recent experimental work,[52] the ground state of Fe−CO is of $^3\Sigma^-$ symmetry, in which our computed Fe−C bond length (1.774 Å) is close to the experimental value (1.798 Å). Two states of Fe−CO were found to be close in energy, the ground state being 2.3 kcal/mol below the metastable structure, in agreement with relativistic calculations reported by Bauschlicher and co-workers[53] (of 0.5 kcal/mol separation). Our energetic separation (2.3 kcal/mol) is closer to the experimental value suggested by Villata and Leopold[54] (≈3.2 kcal/mol) than that reported by Bauschlicher.

High-Spin Complexes. The equilibrium geometries for the low-lying high- and low-spin electronic states of Sc−, Ti−, and V−CO compounds were found to be linear, in agreement with previous calculations.[14,17,20,25,28,55−57] The calculated ground states of Sc−CO and V−CO are of $^4\Sigma^-$ and $^6\Sigma^+$ symmetries, in line with the ESR suggestion.[13,58] The electronic ground state of the Ti−CO compound is found to be of $^5\Delta$ symmetry. According to our calculated bond dissociation energies (BDE in Table 2), relative to the Sc(^{4}F)−, Ti(^{5}F)−, and V(^{6}D)−CO($^1\Sigma^+$) asymptotes, Sc is found to be the most strongly bound, Ti the next most strongly bound, and V the most weakly bound,

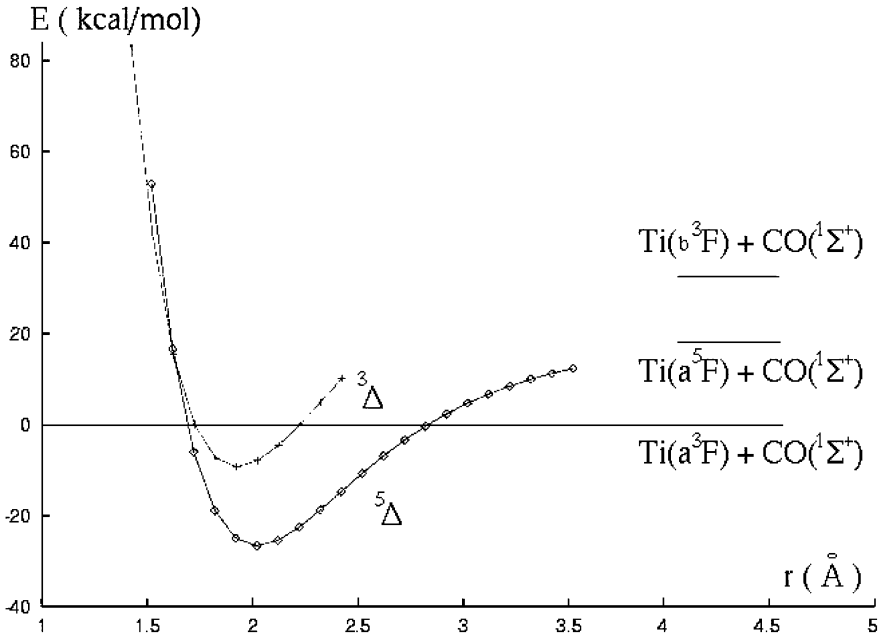

Figure 2. Two low-lying states of Ti−CO.

in agreement with previous high-level calculations.[14] In contrast to the Sc−CO case, the metal−carbon bond length in the low-spin state is shorter than that of the high-spin one. It should be noted that, for the Fe−, Co−, and Ni−CO molecules, the metal−carbon bond length was calculated to be always shorter in the high-spin state than in the low-spin one (ground state). The bond dissociation energies of the high-spin states, with respect to the atomic ground electronic states in taking into account the 4s → 3d promotion energies (Table 1), were found to be −16.8, −26.6, and −20.6 kcal/mol, respectively, for Sc−, Ti−, and V−CO. For the low-spin states of Sc−, Ti−, and V−CO, the bond dissociation energies were calculated to be 8.4, 9.3, and 7.8 kcal/mol, respectively. In previous theoretical works, with a pure nonlocal functional[20] and with the second-order Møller−Plesset (MP2),[57] doublet Sc−CO was predicted to be either unbound or very weakly bound (r_{ScC} > 3.5 Å). Frey and co-workers[57] found a very small donation and back-donation in the doublet state ($^2\Sigma^+$), indicating a very weak interaction between the ground state of Sc(^{2}D) and the carbon monoxide. Nevertheless, according to our calculations, the $^2\Pi$ state of Sc−CO, derived from the Sc ^{2}F($3d^24s^1$) configuration is bound relative to the ground state of Sc by 8.4 kcal/mol, because it has the best π back-bonding. However, both states of these molecules are stable thermodynamically, but the low-spin state corresponds to a metastable complex. This feature is illustrated in Figure 2, in the Ti−CO case.

2.2. Bonding Considerations. The bonding in the transition-metal complexes is classically explained by a simple donor−acceptor mechanism. The strength of the M−CO bond is determined by a balance between π back-donation from the metal to the CO π^* orbital (which could be correlated to the C−O bond length) and σ donation from the carbon lone pair to the vacant orbital of the metal (which could be correlated to the M−C distance). The latter interaction (σ donation) is essentially repulsive. To reduce this repulsion, several mechanisms were suggested.[14,20] In particular, the symmetry of the ground state corresponds to a minimal occupation of the σ orbitals and to a maximal occupation of the π one. Moreover, the multiplicity is lowered with respect to the formal ground state by the spin pairing of some d electrons, which lowers the stabilizing exchange interactions.[20,59] However, these rules are limited and often fail to predict the right configuration of the ground state. The ground state of Cr− and Mn−CO, for instance, is wrongly predicted to belong to the $^5\Sigma^+$ and $^4\Pi$ states. As already pointed out by Frenking and co-workers,[60,61] it is impossible to find a correlation either between the M−C bond length and ligand → metal donation, or between the C−O bond length and metal → ligand back-donation. Therefore, the classical model of the chemical bonding (donation/back-donation on the ground of the individual molecular orbitals) should be regarded as a qualitative scheme to understand some metal−ligand interactions, but not as a quantitative model. It is only the total electron distribution obtained by summing the densities of the electrons in all the molecular orbitals that has a real physical significance, because of the noninvariance of molecular orbitals.

To study the total electron density properties, we have undertaken the topological analysis of the electron density distribution function within the atoms in molecules (AIM) framework[62] and the electron localization function of Becke and Edgecombe.[63]

2.2.1. What Can Be Learned from the AIM Analysis? The AIM analysis enables the estimation of the net electronic transfer from the metal to the carbonyl moiety by integrating the electron density over the metal atomic basin; in addition, the delocalization indexes δ(M,C) introduced by Fradera et al.[64] provide complementary quantitative information on the nature of the metal−carbonyl bond. It is worth recalling that these latter indexes, actually derived from a statistical point of view considering the variance and covariance of the atomic populations, were previously introduced by Cioslowski and Mixon[65] and later (with orbital invariance) by Ángyán et al.[66] as "topological bond orders". Another traditional AIM set of criteria is formed by the values of the density, its laplacian, and the density of energy calculated at the bond critical point, which indicates if the interaction belongs to the closed shell or to the electron shared interaction.

2.2.2. What Can Be Learned from the ELF Analysis? The partition of the molecular space provided by the ELF analysis intends to give a more chemical insight than the AIM one. In particular, the study of the ELF basins is expected to describe how the charge transfer is spread over the carbonyl moiety and

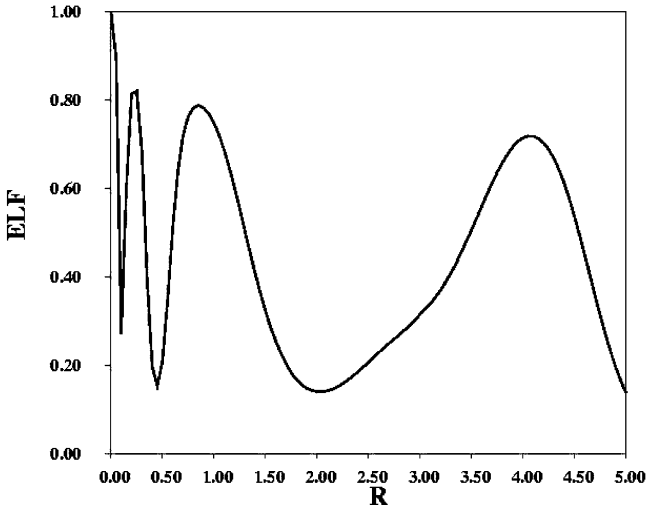

Figure 3. ELF profile for Mn.

also to indicate where the unpaired electrons are localized. The ELF analysis of the M−CO complexes yields seven basins, three core basins, namely, C(M), C(C), and C(O), and four valence basins accounting for the oxygen lone pairs V(O), the CO bond V(C,O), the carbon−metal bond V(M,C), and the free valence of the metal V(M). It is interesting to note that the formation of a M−CO complex corresponds to a global tautomorphic process in the vocabulary introduced by Krokidis et al.[67] because the number of basins is identical in the isolated subunits. Such a process, in which the synaptic order of one basin is increased betokens the formation of a dative bond (see examples in refs 67 and 68). From a rigorous point of view the standard expression of the ELF[63] is only valid for closed-shell systems described by a single determinant. However, it can be used for open-shell systems for which acceptable results have been obtained; for example, it yields similar atomic shell populations compared to those obtained with a spin-polarized formula[69] and realistic populations in the case of radicals.[70]

Chemists generally consider the 3d orbital electrons of transition-metal elements as valence electrons because of the stepwise occupation of these orbitals and of the accessibility of oxidation number greater than 2. The ELF partition associates electron density to core and valence regions. It does not use the orbital concept. The ELF profile of a transition-metal atom such as Mn (Figure 3) evidences a shell structure with three core shells, namely, K, L, and M, and an external valence shell. The minimum of the function before the valence shell determines the core radius, which is 2.07 au.[69] The value of the electron density integrated over the core sphere amounts 22.8 e, whereas the valence shell population is 2.2 e. Therefore, the five "valence" electrons of the traditional representation contribute much more in the topological sense to the core density than to the valence one. For the main group elements Ca and Ga flanking the first series of transition, the core radii are 2.55 and 1.60 au, respectively, and the core radii of the transition-metal elements fall within this range. It is worth noting that the valence shell population is always larger than its expectation (2 or 1), which can be interpreted by leaking from the M shell due to the ambivalent core-valence nature of the d functions in the orbital model. In this paper we will adopt the notation $[Ar]c^x\upsilon^y l^z$ for the electronic configurations of the metal atoms in the complex. [Ar] denotes 9 electron pairs of the core, c the extra core electrons localized within the core that correspond to the d electrons in the delocalized orbital scheme (σ,π,δ), υ the free valence electrons of the metal (σ orbital), and l the electrons transferred to the ligand (π^* orbitals); x, y, and z are the real partial occupancies of the three relevant regions of the molecular space, which satisfy $x + y + z = Z - 18$.

TABLE 3: AIM Analysis of MCO Complexes: Net Atomic Charge q(M), Metal Atom Basin Integrated Spin Projection $\langle S_z \rangle$, Delocalization Index δ(M,C), Electron Density at the Bond Critical Point and Its Laplacian ρ(bcp), ∇^2(bcp), and NBO Net Charge[25] (for All Complexes Except MnCO ROB3LYP Calculations)

M	state	q(M)	$\langle S_z \rangle$	δ(M,C)	ρ(bcp)	∇^2(bcp)	q(M)
Sc	$^4\Sigma^-$	0.71	1.04	1.24	0.0856	0.3657	0.514
	$^2\Pi$	0.39	0.29	0.86	0.0690	0.2194	
Ti	$^5\Delta$	0.59	1.58	1.22	0.0917	0.3989	0.355
	$^3\Delta$	0.46	0.82	0.84	0.0760	2.337	
V	$^6\Sigma$	0.48	2.13	1.20	0.0975	0.4252	0.247
	$^4\Delta$	0.35	1.29	1.10	0.1056	0.3501	
Cr	$^7A'$	0.38	2.71	0.82	0.0732	0.1799	0.228
	$^7\Sigma^+$	0.33	2.73	0.90	0.0759	0.3056	0.164
Mn	$^6\Pi$	0.53	2.64	1.04	0.0958	0.4227	
	$^4\Pi$	0.46	1.72	1.28	0.1287	0.4618	0.300
Fe	$^3\Sigma^-$	0.31	1.0	1.76	0.1947	0.6031	0.180
	$^5\Sigma^-$	0.26	2.34	1.14	0.1216	0.5734	
Co	$^2\Delta$	0.29	0.5	1.14	0.1998	0.6239	0.244
	$^4A'$	0.25	1.34	1.0	0.1129	0.2829	
Ni	$^1\Sigma^+$	0.29		1.74	0.2029	0.6550	0.109
	$^3\Delta$	0.23	0.87	1.12	0.1300	0.3951	
Cu	$^2A'$	0.22	0.36	1.08	0.1277	0.3758	0.181
	$^2\Sigma^+$	0.18	0.44	1.10	0.1313	0.5501	0.076

2.3. Metal−Carbonyl Bonding Analysis. *2.3.1. AIM Analysis.* Table 3 presents the quantitative data of the AIM analysis of the metal−carbonyl interaction, namely, the electron density, laplacian of the electron density at the M−C bond critical point, metal atom net charge, and M−C delocalization index. The common features of the electron density analysis are

(1) the electron transfer from the metal to the carbonyl, which is larger than that previously calculated by Adamo et al.[25] using the NPA approach,

(2) the laplacian of the electron density at the MC bond critical point, which is large and positive, and

(3) the energy density at the same point, which is small and negative.

In all cases the interaction can be characterized as a closed-shell interaction involving a charge transfer; in other words, as expected, the MC bond is a dative bond. However, differences appear that enable us to classify the complexes in three groups consistent with the spin state change.

High-Spin Complexes. The net electron transfer is rather large, i.e., 0.5 ± 0.1 for the three complexes, and the delocalization index is close to 1.2. The electron density at the bond critical point is 0.09, the laplacian ranging from 0.34 to 0.42 .and the energy density on the order of -0.015.

Low-Spin Complexes. In the low-spin complexes the electron transfer is about half that calculated for the high-spin species whereas the delocalization indexes are larger ($\sim$1.6). At the bond critical point the electron density and the laplacian are almost 2 times larger than in the high-spin case. The energy density is also larger in magnitude (~ -0.1).

Conserved Spin Multiplicity Complexes. The spin multiplicity of CrCO, MnCO, and CuCO is the same as in the ground state free metallic atoms. In all complexes the charge transfer is rather low as well as the delocalization index, especially for the two bent complexes CrCO and CuCO. The properties calculated at the bond critical point are similar to those of the high-spin complexes.

For the linear complexes, the variation of the spin multiplicity appears to be the driving force that governs the metal−carbonyl interaction. To this respect, MnCO appears to be intermediate

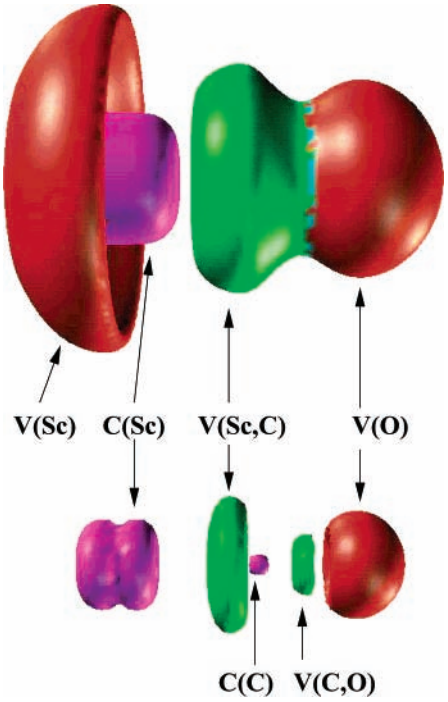

Figure 4. Localization domains of ScCO. The bounding isosurfaces are ELF = 0.30 (top) and ELF = 0.80 (bottom).

between the high- and low-spin complexes, because its charge transfer is close to the low-spin value, whereas the values of the other indicators fall in the high-spin group. The behavior of the two bent complexes is characterized by small charge transfers and delocalization indexes, but it is nevertheless close to that of MnCO.

2.3.2. ELF Analysis. The localization domains of ScCO are displayed in Figure 4, which is representative of the linear complexes. There are three core basins: C(Sc), C(C), and C(O) and four valence basins V(Sc), V(Sc,C), V(C,O), and V(O). The value of ELF at the attractor of V(Sc) is rather low and therefore the associated domain does not exist for ELF = 0.8. The localization reduction diagram[71,72] of all linear complexes displays a unique pattern:

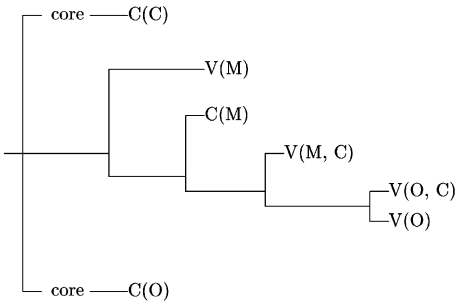

The complex can be considered as a molecule as the first separations occur between the C(C) and C(O) domains from the remaining part. The next separation concerns the V(M) monosynaptic domain, the metal atom core remains in the same reducible domain as the carbonyl valence attractors, this can be interpreted as a result of the ambivalent (core-valence) character of the 3d subshell. After the separation of the C(M) domain, the diagram reflects the electronegativity difference of C and O, this latter atom keeping its valence structure at a rather large ELF value. This can also be understood as the effect of the polarization of the CO bond. In the case of the two bent

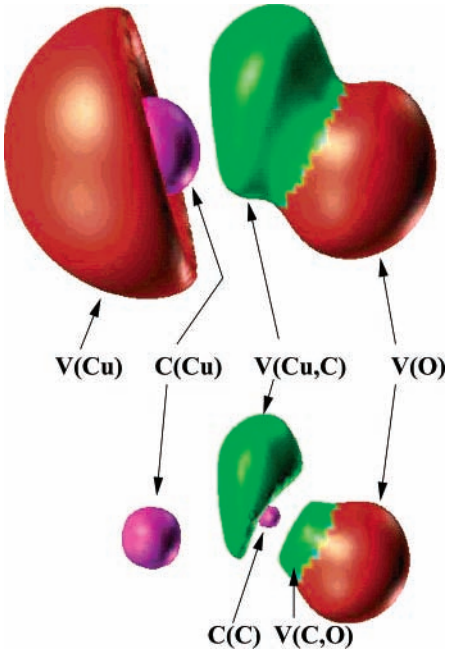

Figure 5. Localization domains of CucCO. The bounding isosurfaces are ELF = 0.30 (top) and ELF = 0.70 (bottom).

structures (for example, CuCO in Figure 5), the localization reduction diagram is quite different:

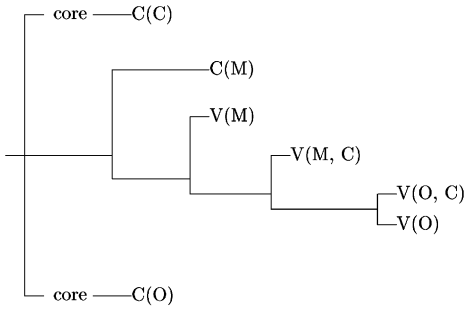

Here, the C(M) domain is separated before the V(M) one, which is consistent with the stability of the d^5 and d^{10} configurations of the metal core; it appears, therefore, that the 3d subshell has less valence character than in the other d^n configurations. Within the ELF analysis the density arising from the d subshell belongs more to the metal core than to the valence. This statement, which is justified by the ELF density partition, is consistent with the traditional assignment of d orbitals in main group elements but is rather unusual for transition metals. However, this does not imply that the d basis function does not participate in the bonding in the actual approximate expansion of the wave function. The ambivalent contribution of the d basis functions is testified by the variance of the C(M) and V(M) populations.

Table 4 gathers the ELF population analysis of the nine complexes in their ground state and in their first excited states.

As in all cases the CO moiety appears to be a well-defined chemical subunit, it is convenient to introduce the net electronic transfer from the metal atom to CO as the difference of the atomic number of the metal and of the sum of the core C(M) and monosynaptic valence V(M) basin populations, i.e.

$$\delta q = Z - \bar{N}(C(\mathrm{M})) - \bar{N}(V(\mathrm{M})) \qquad (1)$$

High-Spin Complexes. The population analysis of the high-spin complexes in their ground state is characterized by the

TABLE 4: ROB3LYP/6-311G(2d) Basin Populations $\bar{N}$, Integrated Half-Spin Densities $\langle S_z \rangle$, Population Differences with Respect to Free Carbon Monoxide Δ, and Net Electron Density Transfer toward Ligand δq

		C(M)		*V*(M)		*V*(C,M)			*V*(C,O)		*V*(O)		
M	state	$\bar{N}$	$\langle S_z \rangle$	$\bar{N}$	$\langle S_z \rangle$	$\bar{N}$	$\langle S_z \rangle$	Δ	$\bar{N}$	Δ	$\bar{N}$	Δ	δq
Sc	$^4\Sigma^-$	19.11	0.57	0.86	0.39	3.46	0.39	0.90	2.56	−0.47	4.78	0.56	1.03
	$^2\Pi$	18.73	0.23	1.78	0.04	2.96	0.16	0.40	2.82	−0.21	4.44	2.22	0.49
Ti	$^5\Delta$	20.24	1.12	0.80	0.36	3.31	0.40	0.34	2.61	−0.42	4.74	0.52	0.96
	$^3\Delta$	19.76	0.68	1.75	0.12	2.86	0.14	0.30	2.90	−0.13	4.40	0.18	0.49
V	$^6\Sigma$	21.59	1.76	0.52	0.24	3.20	0.31	0.64	2.68	−0.35	4.70	0.48	0.89
	$^4\Delta$	20.77	1.10	1.68	0.14	2.92	0.18	0.36	2.89	−0.14	4.44	0.22	0.55
Cr	$^7A'$	23.0	2.46	0.40	0.19	3.14	0.24	0.58	2.65	−0.38	4.59	0.37	0.60
	$^7\Sigma^+$	22.57	2.26	0.90	0.42	2.99	0.24	0.43	2.86	−0.17	4.48	0.26	0.53
Mn	$^6\Pi$	23.09	2.14	0.98	0.43	3.40	−0.04	0.84	2.61	−0.42	4.68	0.46	0.93
	$^4\Pi$	22.95	1.84	1.14	−0.15	3.32	−0.10	0.76	2.65	−0.38	4.70	0.48	0.91
Fe	$^3\Sigma^-$	23.83	0.91	1.08	0.06	3.42	0.03	0.86	2.65	−0.38	4.79	0.57	1.09
	$^5\Sigma^-$	24.19	1.81	1.02	0.44	3.26	0.40	0.70	2.82	−0.21	4.47	0.25	0.79
Co	$^2\Delta$	25.50	0.48	0.41	0.02	3.46	0.00	0.90	2.63	−0.40	4.77	0.55	1.09
	$^4A'$	25.76	1.15	0.71	0.16	3.03	0.12	0.47	2.75	−0.28	4.52	0.30	0.53
Ni	$^1\Sigma^+$	26.70		0.28		3.37		0.81	2.66	−0.37	4.78	0.56	1.02
	$^3\Delta$	26.68	0.68	0.62	0.18	3.18	0.10	0.62	2.74	−0.29	4.55	0.33	0.70
Cu	$^2A'$	27.86	0.18	0.52	0.18	3.12	0.09	0.56	2.73	−0.30	4.52	0.30	0.62
	$^2\Sigma^+$	27.80	0.20	0.65	0.24	2.94	0.04	0.38	2.95	−0.08	4.40	0.18	0.55

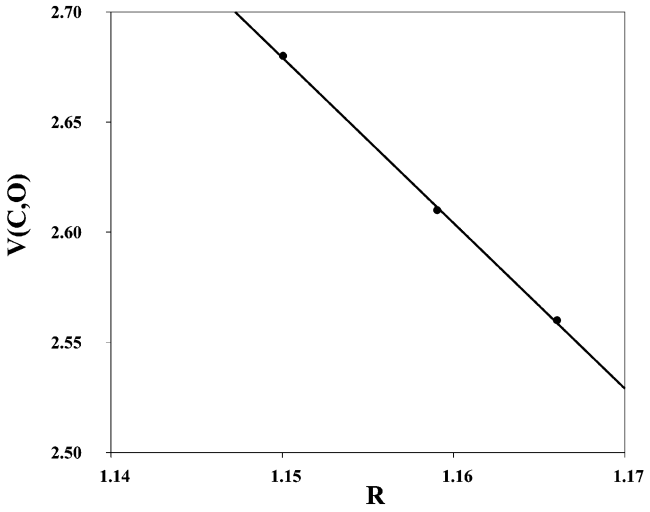

Figure 6. *V*(C,O) population in au vs CO internuclear distance in Å.

decrease of the net charge transfer with the increase of the metal atomic number or, said in other words, with the increase of the metal atom electronegativity, which is consistent with basic chemical intuition. As a consequence, the absolute variations of the V(C,M), V(C,O), and V(O) populations with respect to uncomplexed carbon monoxide behave consistently. Moreover, as displayed in Figure 6, the CO internuclear distance is nicely correlated to the V(C,O) population. Another interesting feature of the high-spin complexes is the distribution of the spin density over the C(M), V(M), and V(C,M) basins. This is not due to the lack of self-interaction correction in the DFT scheme because very close values of the integrated spin density over these basins are calculated at the Hartree−Fock (restricted open-shell) level. The integrated spin densities in the $M_S = S$ state (1.14, 2.24, and 3.52 for Sc, Ti, and V, respectively) suggest that the local core configurations are dominated by the $[Ar]d^1$, $[Ar]d^2$, and $[Ar]d^3$ configurations, the weight of the remaining $[Ar]d^2$, $[Ar]d^3$, and $[Ar]d^5$ increasing with *Z*. The trends of the basin populations of FeCO($^5\Sigma^-$) and NiCO($^3\Delta$) are consistent with those previously described for ScCO, TiCO, and VCO, except that the V(C,O) population in NiCO is less than that in FeCO. The local configurations of the metallic cores are dominated by the $[Ar]d^6$ and $[Ar]d^9$ configurations. It is possible to propose an occupation scheme in terms of the occupancy of C(M) and V(M) and of the net transfer to the ligand written as $c^x v^y l^z$ in which *c*, *v*, and *l* stand for C(M), V(M), and the transferred charge. The real *x*, *y*, and *z* values can be then interpreted as arising from resonance contributions with integer values. The multiplicity is given by Hund's rule by considering the core configuration $[Ar]c^{n+2}$ where $n = Z - 20$. Therefore in the high-spin case the most probable resonance structures that are consistent with the spin multiplicity are $[Ar]c^{n+2}$, $[Ar]c^{n+1}v^1$, $[Ar]c^{n+1}l^1$, $[Ar]c^n l^2$, and $[Ar]c^{n-1}v^1l^2$. As the ground states of ScCO, TiCO, and VCO belong respectively to the Σ, Δ, and Σ irreducible representations, the occupancy of *l* must be 0 or 2, whereas that of *v* should be either 0 or 1. For example, the following tentative weights enable us to recover the populations and integrated spin densities of C(M) and V(M) and the transferred charge:

ScCO	$[Ar]c^3$ (14%)	$[Ar]c^2v^1$ (32%)	$[Ar]v^1l^2$ (54%)
TiCO	$[Ar]c^4$ (20%)	$[Ar]c^3v^1$ (32%)	$[Ar]c^1v^1l^2$ (48%)
VCO	$[Ar]c^5$ (48%)	$[Ar]c^4v^1$ (8%)	$[Ar]c^2v^1l^2$ (44%)

The weight of the $[Ar]c^{n+2}$ limit structure increases with *Z* whereas that of $[Ar]c^{n-1}v^1l^2$ undergoes the opposite trend.

Conserved Spin Multiplicity Complexes. Only MnCO whose ground state is $^6\Pi$ can be directly compared with the other linear complexes. The main difference from the high-spin complexes is that there is no spin density in the V(C,Mn) basin. The populations and integrated spin densities of C(Mn) are consistent with a resonance picture involving the two configurations $[Ar]c^6v^1$ (53%) and $[Ar]c^4v^1l^2$ (47%).

In the bent structures, the local core configurations are $[Ar]c^5$ and $[Ar]c^{10}$ for CrCO and CuCO, respectively. As shown in Figure 7, the ∠OCM is such as the electron density transfer from the metal is maximized. This transfer occurs mostly between the V(M) and V(C,M) basins and, as a consequence, the remaining spin density is shared between them.

Low-Spin Complexes. The net electron density transfer δq is on the order of 1 *e* for FeCO, CoCO, and NiCO in their ground state and about half for the excited states of ScCO, TiCO, and VCO. The V(M) populations of these three latter complexes are greater than 1.5 *e* whereas the core populations are less than their expectations (i.e., 18.73 for Sc, 19.76 for Ti, and 20.77 for V). The behavior of Co and Ni is different because their V(M) populations are less than 0.5 *e* and their core populations are larger than the expectations. Fe follows the expectation, i.e., $\bar{N}(C(Fe)) \sim 24$, $\bar{N}(V(Fe)) \sim 1$. For the $M_S = S$ components of the multiplets, the spin density is essentially located in the C(M)

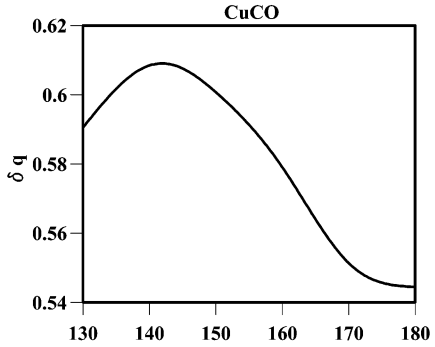

Figure 7. Total charge transfer vs bent angle in the CuCO complex.

basin above all for Fe and Co. As in the high-spin case, the multiplicity is given by Hund's rule applied to the [Ar]c^{n+2} configuration. The other configurations consistent with this multiplicity are thus [Ar]$c^n v^2$ and [Ar]$c^{n-2}l$.[4] As there is no spin density within the CO moiety, the l occupancy should be 0 or 4; for the same reason, that of v is 0 or 2. Possible weights of these configurations are

FeCO	[Ar]c^8 (25%)	[Ar]c^6v^2 (50%)	[Ar]c^4l^4 (25%)
CoCO	[Ar]c^9 (55%)	[Ar]c^7v^2 (20%)	[Ar]c^5l^4 (25%)
NiCO	[Ar]c^{10} (61%)	[Ar]c^8v^2 (14%)	[Ar]c^6l^4 (25%)

Core Shapes and Geometries. The local core configurations of the bent structures, as given by the population and integrated spin density of the core basins, are ^{6}S and ^{1}S for Cr and Cu, respectively. For linear structures, the combination of the core population and core spin density is never consistent with a local S state but rather with P or D. Around the Cr and Cu core, the ELF function has a local spherical symmetry whereas for the other atoms it is cylindrical. In this latter case, the Pauli repulsion between V(C,M) and C(M) and V(M) is minimized in the linear geometry where V(C,M) and V(M) are in opposition with respect to C(M).

In the bent complexes the ELF function around the metal nucleus has a local spherical symmetry and therefore the molecular axis of the ligand is not a preferred direction for the core symmetry. Moreover, the density available for the transfer belongs entirely to V(M) at infinite distance and the transfer is made easier when the distance between the V(C,M) and V(M) attractors is decreased.

2.4. Estimate of Topological Donation and Back-Donation. Within the Dewar−Chatt−Duncanson scheme, the donation is defined as an electronic transfer from the ligand toward the metal that involves the canonical orbitals of symmetry σ. The back-donation is the contribution of the π canonical orbitals to an electronic transfer in the opposite direction. As the topological partitions enable us to distinguish metal and ligand moieties, it is possible to estimate quantitatively the donation and the back-donation by considering the contributions of the orbitals of each symmetry to the localization basins of one of the moieties. Consider, for example, the ScCO complex and the AIM partition. The sum of the σ orbitals to the carbon and oxygen atomic basins is 9.86 e instead of 10 and therefore the AIM σ-donation is 10.0−9.86 = 0.14 e. The π-back-donation is 0.78 e because the π orbitals contribute 4.78 e to ligand atomic basins.

The analysis of ELF yields a different set of values because the whole V(C,M) basin is assigned to the ligands according to its appearance in the bifurcation diagram whereas in the AIM partition it is shared between the metal and carbon atomic basins. We have therefore to consider the σ and π contributions to the C(C), C(O), V(C,M), V(C,O), and V(O) basins. For the ScCO complex, the donation amounts to −0.03 (it is in fact a back-donation) and the back-donation to 1.02 e.

TABLE 5: AIM, ELF, and NBO[25] Donations and Back-Donation of the Linear MCO High-Spin and Low-Spin Complexes in Their Ground State

	donation			back-donation		
	AIM	ELF	NBO	AIM	ELF	NBO
ScCO	0.14	−0.03	0.171	0.78	1.05	0.339
TiCO	0.17	0.02	0.188	0.69	0.87	0.273
VCO	0.21	0.08	0.201	0.64	0.82	0.230
FeCO	0.42	−0.02	0.300	0.68	1.08	0.245
CoCO	0.41	0.0	0.313	0.67	1.09	0.281
NiCO	0.41	0.06	0.347	0.68	1.06	0.230

The AIM and ELF donations and back-donations of the linear ground-state complexes are listed in Table 5. As a general rule the ELF partition yields negligible donation values and therefore the back-donation represents almost the whole charge transfer. The AIM back-donation is always on the order of 0.7 ± 0.1 whereas the donation is on the order of 0.17 ± 0.04 for the high-spin complexes and 0.41 for the low-spin ones. With respect to the NBO analysis of Adamo and Lelj,[25] the AIM net charge on the metal atom is always larger, which is consistent with the M^+CO^- picture. Consequently, the AIM values of donation and back-donation are also larger. The picture obtained from the ELF partition scheme supports the M^+CO^- structure.

3. Conclusions

The formation of a MCO complex in which M is a transition-metal atom of atomic number $Z = 20 + n$ obeys the following rules:

1. Except for $n = 4, 5, 9$, the spin multiplicity obeys Hund's rule for the configuration [Ar]c^{n+2}.

2. The averaged local configuration of the core is [Ar]c^n, except for Cr and Cu for which it is [Ar]c^{n+1}, as expected from the electronic configuration of the ground state of the free atom.

3. For $n < 4$ the stable configuration multiplicity is $n + 3$. Because the local core configuration is mostly [Ar]c^n, two unpaired electrons can be shared by the metal valence basin, the ligand, and the metal core. Therefore the total charge transfer and the V(M) population are both close to 1. Moreover, the integrated spin densities over V(M) and V(C, M) are also close to 1.

4. For $n = 5$, the interaction in the ground state can be described in terms of two resonance structures: one with 4 unpaired electrons in C(Mn), one in V(Mn) and a pair transferred to the ligand, the other with 6 electrons in C(Mn) and one in V(Mn).

5. For $n > 5$ the ground-state multiplicity is $9 - n$. One electron pair can be shared by the ligand, V(M) and in part C(M). There is no spin density within V(M) and V(C,M). δq is close to 1 and the V(M) population is less than 1.

6. For Cr and Cu, the ELF function is spherically symmetrical in the core region of the metal, only one electron can be distributed over V(M) and V(M,C). The charge transfer from the metal is maximized for a bent structure.

7. For all other metals, the local symmetry of ELF in the metal core is cylindrical, which favors the linear geometry of the complex.

8. In the case of linear complexes it is possible to estimate the donation and back-donation contribution to the net charge transfer. In the ELF analysis the donation contribution is almost negligible.

Acknowledgment. We thank Dr. Alain Sevin for his constant support and stimulating discussion and Dr. H. Gérard for critical reading of the draft manuscript.

References and Notes

(1) Joly, H. A.; Manceron, L. *Chem. Phys.* **1998**, *226*, 61.
(2) Tremblay, B.; Manceron, L. *Chem. Phys.* **1999**, *242*, 235.
(3) Chenier, J. H. B.; Hampson, C. A.; Howard, J. A.; Mile, B. *J. Phys. Chem.* **1988**, *92*, 2745.
(4) Chenier, J. H. B.; Hampson, C. A.; Howard, J. A.; Mile, B. *J. Phys. Chem.* **1989**, *93*, 114.
(5) Chenier, J. H. B.; Howard, J. A.; Joly, H. A.; Tomieto, M. *Can. J. Chem.* **1989**, *67*, 655.
(6) Huber, H.; Kündig, E. P.; Moskovits, M.; Ozin, G. A. *J. Am. Chem. Soc.* **1975**, *97*, 2097.
(7) Hanlan, L.; Huber, H.; Ozin, G. A. *Inorg. Chem.* **1976**, *15*, 2592.
(8) McIntosh, D.; Ozin, G. A. *J. Am. Chem. Soc.* **1976**, *98*, 3167.
(9) McIntosh, D.; Ozin, G. A. *Inorg. Chem.* **1977**, *16*, 51.
(10) Kasai, P. H.; Jones, P. M. *J. Am. Chem. Soc.* **1985**, *107*, 813.
(11) Kasai, P. H.; Jones, P. M. *J. Phys. Chem.* **1985**, *89*, 1147.
(12) Kasai, P. H.; Jones, P. M. *J. Am. Chem. Soc.* **1985**, *107*, 6385.
(13) Van Zee, R. J.; Bach, S. B. H.; Weltner, W., Jr. *J. Phys. Chem.* **1986**, *90*, 583.
(14) Barnes, L. A.; Bauschlicher, Jr., C. W. *J. Chem. Phys.* **1989**, *91*, 314.
(15) Smith, G. W.; Carter, E. A. *J. Phys. Chem.* **1991**, *95*, 2327.
(16) Mattar, S. M.; Hamilton, W. *J. Mol. Struct. (THEOCHEM)* **1991**, *226*, 147.
(17) Jeung, G. *J. Am. Chem. Soc.* **1992**, *114*, 3211.
(18) Sodupe, M.; Bauschlicher, C. W., Jr.; Lee, T. J. *Chem. Phys. Lett.* **1992**, *189*, 266.
(19) Marian, C. M. *Chem. Phys. Lett.* **1993**, *215*, 582.
(20) Fournier, R. *J. Chem. Phys.* **1993**, *98*, 8041.
(21) Fournier, R. *J. Chem. Phys.* **1993**, *99*, 1801.
(22) Bauschlicher, C. W., Jr. *J. Chem. Phys.* **1994**, *100*, 1215.
(23) Barone, V. *Chem. Phys. Lett.* **1995**, *233*, 129.
(24) Barone, V. *J. Phys. Chem.* **1995**, *99*, 11659.
(25) Adamo, C.; Lelj, F. *J. Chem. Phys.* **1995**, *103*, 10605.
(26) Chung, S.-C.; Krüger, S.; Pacchioni, G.; Rösch, N. *J. Chem. Phys.* **1995**, *102*, 3695.
(27) Schwerdtfeger, P.; Bowmaker, G. A. *J. Chem. Phys.* **1994**, *100*, 4487.
(28) Jeung, G.; Haettel, S. *Int. J. Quantum Chem.* **1997**, *61*, 547.
(29) Dewar, M. J. S. *Bull. Soc. Chim. Fr.* **1951**, *18*, C71.
(30) Chatt, J.; Duncanson, L. A. *J. Chem. Soc.* **1953**, 2939.
(31) Frisch, M. J.; Trucks, G. W.; Schlegel, H. B.; Scuseria, G. E.; Robb, M. A.; Cheeseman, J. R.; Zakrzewski, V. G.; Montgomery, J. A., Jr.; Stratmann, R. E.; Burant, J. C.; Dapprich, S.; Millam, J. M.; Daniels, A. D.; Kudin, K. N.; Strain, M. C.; Farkas, O.; Tomasi, J.; Barone, V.; Cossi, M.; Cammi, R.; Mennucci, B.; Pomelli, C.; Adamo, C.; Clifford, S.; Ochterski, J.; Petersson, G. A.; Ayala, P. Y.; Cui, Q.; Morokuma, K.; Malick, D. K.; Rabuck, A. D.; Raghavachari, K.; Foresman, J. B.; Cioslowski, J.; Ortiz, J. V.; Baboul, A. G.; Stefanov, B. B.; Liu, G.; Liashenko, A.; Piskorz, P.; Komaromi, I.; Gomperts, R.; Martin, R. L.; Fox, D. J.; Keith, T.; Al-Laham, M. A.; Peng, C. Y.; Nanayakkara, A.; Challacombe, M.; Gill, P. M. W.; Johnson, B.; Chen, W.; Wong, M. W.; Andres, J. L.; Gonzalez, C.; Head-Gordon, M.; Replogle, E. S.; Pople, J. A. *Gaussian 98*; revision A.9; Gaussian Inc.: Pittsburgh, PA, 1998.
(32) Becke, A. D. *J. Chem. Phys.* **1993**, *98*, 5648.
(33) Lee, C.; Yang, W.; Parr, R. G. *Phys. Rev. B* **1988**, *37*, 785.
(34) Krishnan, R.; Binkley, J. S.; Seeger, R.; Pople, J. A. *J. Chem. Phys.* **1980**, *72*, 650.
(35) Clark, T.; Chandrasekhar, J.; Spitznagel, G. W.; Schleyer, P. V. R. *J. Comput. Chem.* **1983**, *4*, 294.
(36) Frisch, M. J.; Pople, J. A.; Binkley, J. S. *J. Chem. Phys.* **1984**, *80*, 3265.
(37) Schaefer, A.; Horn, H.; Ahlrichs, R. *J. Chem. Phys.* **1992**, *97*, 2571.
(38) Schaefer, A.; Huber, C.; Ahlrichs, R. *J. Chem. Phys.* **1994**, *100*, 5829.
(39) Andrae, D.; Haeussermann, U.; Dolg, M.; Stoll, H.; Preuss, H. *Theor. Chim. Acta* **1990**, *77*, 123.
(40) Silvi, B.; Savin, A. *Nature* **1994**, *371*, 683.
(41) Noury, S.; Krokidis, X.; Fuster, F.; Silvi, B. *Comput. Chem.* **1999**, *23*, 597.
(42) Zhou, M.; Andrews, L. *J. Chem. Phys.* **1999**, *111*, 4548.
(43) Ozin, G. A.; Vander Voet, A. *Prog. Inorg. Chem.* **1975**, *19*, 137.
(44) Bach, S. B. H.; Taylor, C. A.; Van Zee, R. J.; Vala, M. T.; Weltner, W., Jr. *J. Am. Chem. Soc.* **1986**, *108*, 7104.
(45) Blitz, M. A.; Mitchell, S. A.; Hackett, P. A. *J. Phys. Chem.* **1991**, *95*, 8719.
(46) Parnis, J. M.; Mitchell, S. A.; Hackett, P. A. *J. Phys. Chem.* **1990**, *94*, 8152.
(47) Mitchell, S. A. In *Gas-Phase Metal Reactions*; Fontijn, A., Ed.; Elsevier Science: Amsterdam, 1992; pp 227−252.
(48) Williams, A. P.; Van Zee, R. J.; Weltner, W., Jr. *J. Am. Chem. Soc.* **1996**, *118*, 4498.
(49) Huber, H.; Kündig, E. P.; Ozin, G. A.; Poe, A. *J. Am. Chem. Soc.* **1975**, *97*, 308.
(50) Andrews, L.; Zhou, M.; Wang, X.; Bauschlicher, C. W., Jr. *J. Phys. Chem. A* **2000**, *104*, 8887.
(51) Bauschlicher, C. W., Jr. *Chem. Phys. Lett.* **1996**, *249*, 244.
(52) Tanaka, K.; Tachikawa, Y.; Tanaka, T. *Chem. Phys. Lett.* **1997**, *281*, 285.
(53) Barnes, L. A.; Rosi, M.; Bauschlicher, C. W., Jr. *J. Chem. Phys.* **1991**, *94*, 2031.
(54) Villata, P. W.; Leopold, D. G. *J. Chem. Phys.* **1993**, *98*, 7730.
(55) Berthier, G.; Daoudi, A.; Suard, M. *J. Mol. Struct. (THEOCHEM)* **1988**, *179*, 407.
(56) Daoudi, A.; Suard, M.; Barthelat, J. C.; Berthier, G. *C. R. Acad. Sci. Paris* **1988**, *306*, 1337.
(57) Frey, R. F.; Davidson, E. R. *J. Chem. Phys.* **1989**, *90*, 5541.
(58) Van Zee, R. J.; Weltner, W., Jr. *J. Am. Chem. Soc.* **1989**, *111*, 4519.
(59) Daoudi, A.; Suard, M.; Berthier, G. *J. Mol. Struct. (THEOCHEM)* **1990**, *210*, 139.
(60) Ehlers, A. W.; Dapprich, S.; Vyboishchikov, S. F.; Frenking, G. *Organometallics* **1996**, *15*, 105.
(61) Frenking, G.; Fröhlich, N. *Chem. Rev.* **2000**, *100*, 717.
(62) Bader, R. F. W. *Atoms in Molecules: A Quantum Theory*; Oxford University Press: Oxford, U.K., 1994.
(63) Becke, A. D.; Edgecombe, K. E. *J. Chem. Phys.* **1990**, *92*, 5397.
(64) Fradera, X.; Austen, M. A.; Bader, R. F. W. *J. Phys. Chem. A* **1998**, *103*, 304−314.
(65) Çioslowski, J.; Mixon, S. T. *Inorg. Chem.* **1993**, *32*, 3209−3216.
(66) Ángyán, J. G.; Loos, M.; Mayer, I. *J. Phys. Chem.* **1994**, *98*, 5244−5248.
(67) Krokidis, X.; Noury, S.; Silvi, B. *J. Phys. Chem. A* **1997**, *101*, 7277−7282.
(68) Boily, J. *J. Phys. Chem. A* **2002**, *106*, 4718−4724.
(69) Kohout, M.; Savin, A. *Int. J. Quantum Chem.* **1996**, *60*, 875.
(70) Catalayud, M.; Andrés, J.; Beltrán, A.; Silvi, B. *Theor. Chem. Acc.* **2001**, *105*, 299.
(71) Savin, A.; Silvi, B.; Colonna, F. *Can. J. Chem.* **1996**, *74*, 1088.
(72) Calatayud, M.; Andrés, J.; Beltrán, A.; Silvi, B. *Theor. Chem. Acc.* **2001**, *105*, 299−308.